SUPERLATTICE WITH ELECTRON QUASI-LOCALISED STATES IN UNIT CELL

A.V. DMITRIEV, V.V. MAKEEV
Department of Low Temperature Physics, the Faculty of Physics, Moscow State University, Moscow, 119899, Russia; dmitriev@lt.phys.msu.su

ABSTRACT

We studied theoretically the electron spectrum and infrared transitions in a superlattice with a unit cell allowing for quasi-localised carrier states. The dispersion relation and the band structure of such a system have been found. We also calculated the dipole matrix element for inter-subband carrier infrared transitions. The wave functions and the electron spectrum in this superlattice show a peculiarity when the energy of a band state approaches the energy of the quasi-localised state in the single cell. In particular, the absorption strength peaks up at the respective frequencies.

INTRODUCTION

Usually, one assumes that in semiconductors, along with other crystals, an electron state belongs to one of the two possible kinds. Namely, it can be either a Bloch band state, or a localised state residing in the forbidden gap. However, a third kind of carrier states, resonant or quasi-localised [1], has been shown to play a significant role in a number of occasions. These states, long before known both in optics [2] and in quantum mechanics [3], appear in semiconductors, e.g. when an impurity level, split off from one band, overlaps with another allowed band, or when a deep impurity level overlaps with one of the allowed energy bands. In certain conditions resonant states may significantly affect the kinetic properties of a semiconductor [4, 5].

Quasi-localised states may be present in artificially prepared heterostructures, e.g. in two-barrier quantum well systems. We have shown earlier [6] that in their presence the absorption coefficient significantly increases in the frequency range of the intraband transitions into the resonant state. Since the latter state formally belongs to the continuum, one can expect it to decay easily into a delocalised wave, so that no strong electric field would be required to add the excited electron to an observable photocurrent. Hence heterostructures with quasi-localised states sound quite appealing as candidates for selective quantum well infrared photodetectors (QWIPs). These detectors would combine high spectral selectivity with low dark current because of low bias applied. Such combination is hardly attainable with conventional QWIPs, where the working transition goes to a bound state, or in the opposite case, to a plain continuum state (see the review article [7]).

In the cited paper [6] we discussed a single quantum well system. However, arrays of quantum wells or superlattices are normally used for experimental purposes and practical applications. Thus we thought it relevant to consider a periodic structure composed of quantum wells with resonant states. This is the goal of the present paper.

The theoretical approach to the electronic spectrum of superlattices is well developed (see e.g. [8, 9]). In [10] a detailed spectral analysis of a conventional superlattice with two alternating layers has been demonstrated. We use a similar approach to analyse the electronic spectrum of a superlattice with a more complex unit cell.

We consider one non-degenerate band, let it be the conduction band, of a semiconductor superlattice, where each cell is described within the effective-mass approximation by a one-dimensional model potential as follows (see also Fig. 1):

$$U(x) = \left\{ \begin{array}{ll} -V, & 0 < x < a \\ 0, & a < x < b \end{array} \right\} + \Omega\,[\delta(x) + \delta(x-a)], \qquad (1)$$

where x is the growth direction of the superlattice, a and b are the well width and the structure period, respectively, V is the well depth. δ-like barriers on the well's edges represent a simplified approximation of additional real barriers of finite width and height that would surround each well. The parameter Ω thus represents to the reverse tunnel transparency of the real barrier. The main barriers of width $(b-a)$ separate the wells. The potential in eq. (1) is assumed to be 0 at the top of the main barrier.

If all the structure consisted of only one quantum well with the potential (1), we might speak of quasi-localised electronic states in its spectrum. These states appear on an energy scale close to truly localised states that would exist in the well, if the additional barriers (walls) were absolutely impenetrable. Finite penetrability of the walls transforms the truly localised size-quantised states into quasi-localised states. Of course, this matters only for the excited states lying above the top of the main barriers, like the two higher levels in Fig. 1. The lower ground state in the single quantum well is always localised.

The δ-function approximation of real barriers adopted in eq. (1) is a well-known simplified method used for example in the Kronig–Penney model of crystal and in other quantum-mechanical problems [11]. It corresponds to a very high and narrow barrier with finite penetrability. From the point of view of the problem we consider here, the main difference between the δ-barrier and the real one is an infinite height of the former. As a result, our model system has an infinite set of quasi-localised states (resonances) whereas a real structure hardly can produce more than one or two of them. But as far as we are interested in properties of a single resonance, the δ-approximation leads to qualitatively correct and physically meaningful results.

Turning back to the periodic heterostructure, let us see how the resonant states affect the properties of the whole system. The envelope wave functions may be represented as:

$$\Psi(x) = \left\{ \begin{array}{ll} A_1 e^{iqx} + A_2 e^{-iqx}, & 0 < x < a \\ B_1 e^{i\kappa x} + B_2 e^{-i\kappa x}, & a < x < b \end{array} \right. ; \quad \Psi(x+b) = e^{ikb}\Psi(x), \qquad (2)$$

where $q = (1/\hbar)\sqrt{2m(E+V)}$, $\kappa = (1/\hbar)\sqrt{2mE}$, E is the particle energy counted from the top of the main barrier, m is the effective mass, kb is the phase shift of the envelope function, resulting from a one-lattice-period displacement along the growth direction. Ignoring the changes in the effective mass across the superlattice layers, we obtain a conventional boundary condition on the left-hand border of the well ($x = 0$):

$$\Psi(x)\big|_{0-}^{0+} = 0, \quad \frac{d}{dx}\ln\Psi(x)\Big|_{0-}^{0+} = \Omega.$$

Having written similar boundary conditions for the right-hand border ($x = a$), we come to a homogeneous system of equations defining the coefficients in eq. (2). A non-zero solution of this system exists only if the system determinant is zero, hence we obtain the dispersion

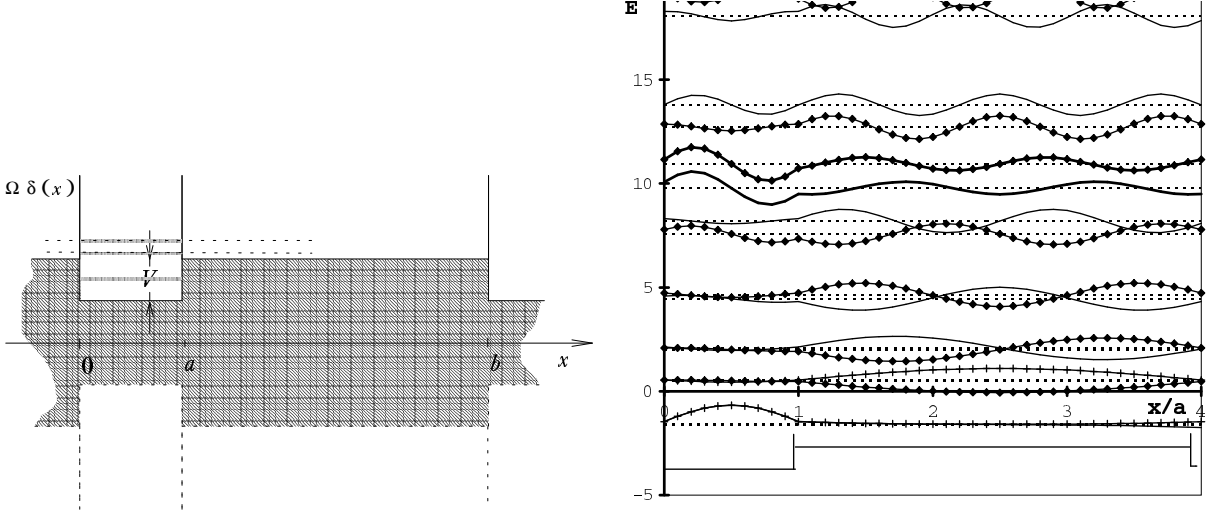

Figure 1: The considered model potential. Several lower subbands are marked. Shadow area corresponds to the energy gap.

Figure 2: The subband structure of the superlattice for $b/a = 4$ and $V = 1.47$. The energy unit is $\hbar^2/ma^2$. The subband edges are marked by horizontal dotted lines. Solid curves represent the envelope functions at the band edges, of which the states with $k = 0$ are marked with rhombuses. Two thick solid curves denote the functions of the 'resonant' subband. The unit cell potential is shown below.

relation:

$$\cos kb = \frac{\Omega^2 - q^2 - \kappa^2}{2\kappa q}\sin\kappa(b-a)\sin qa + \frac{\Omega}{q}\cos\kappa(b-a)\sin qa + \frac{\Omega}{\kappa}\sin\kappa(b-a)\cos qa + \cos\kappa(b-a)\cos qa. \quad (3)$$

The energy intervals where the absolute value of the right-hand side of eq. (3) does not exceed unity, correspond to allowed subbands of our superlattice. Unfortunately, no analytic solution for the wave function coefficients in eq. (2) can be obtained at arbitrary k, so further spectrum calculations were performed numerically.

RESULTS

Spectrum, Wave Functions and Momentum Matrix Element

Fig. 2 depicts the envelope wave functions of several adjacent subbands. The lower plot represents a wave function belonging to the lowest subband; this band originates from the well's ground state. Naturally, electronic density concentrates within the well's limits. The shape of the wave functions in the unit cell does not depend on k; only the phase shift between adjacent cells changes with k.

The rest of the wave functions in Fig. 2 corresponds to positive energy values. Most of these have electronic density concentrated just outside the wells. We can roughly infer that these functions originate from electronic states residing over the barriers. The walls (additional barriers), surrounding the wells, prevent the particles from entering the wells.

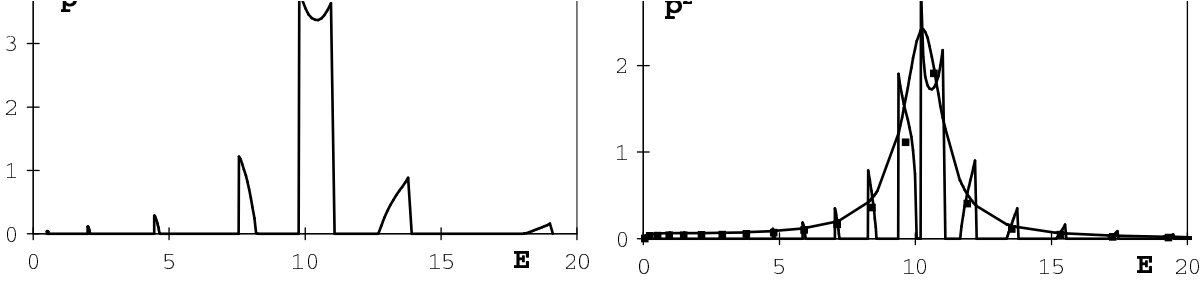

Figure 3: The momentum matrix element squared measured in $\hbar^2/a^2$ for the same system as in Fig. 2. The energy unit is $\hbar^2/(ma^2)$.

Figure 4: The same dependence as in Fig. 3, but for thicker main barriers: $b/a = 10$. The well depth $V = 1.47$. Full squares show the ratio of $\langle|p_n|^2\rangle/(E_n - E_{n-1})$ for the superlattice. The smooth curve represents $|p_{if}|^2\rho$ in a single quantum well according to [6].

Note that functions on the edges of each subband have definite parity when viewed from both well centre or barrier centre. Further on we speak of parity according to the well centre. These functions have different parities on the opposite edges of each subband.

However, there is one subband, with energy close to the resonant value, where the functions do not obey the latter rule. Let us call this band resonant. Here electronic density is large within the well limits, and the envelope functions have the same parity on the band edges. Their structure resembles the structure of the functions in the lowest subband, which originated from the localised states in the wells. Henceforth we can expect the dipole matrix element of optical transition between these two bands to be anomalously large, because of high overlap between the wave functions in the two bands. Then the absorption coefficient would also increase. The energy of corresponding transitions in common superlattices lies in the infrared range.

In our calculations we used $|p_n(k)|^2$, the momentum matrix element squared, as a convenient straightforward parameter, characterising the absorption per one electron in the ground subband (see below). $|p_n(k)|^2$ is the matrix element between wave functions in the lowest and n-th subbands taken at one Bloch vector value k (because of negligible photon's momentum, we can consider the electron transitions vertical). The derivative parameters, such as absorption probability or absorption coefficient α, are proportional to $|p_n(k)|^2$.

Figures 3 and 4 depict the dependence of $|p_n|^2$ on the energy of the final electron state at two different values of superlattice period. The variation of other superlattice parameters (a, Ω, V) does not change the qualitative picture. We can see first that the transition matrix element goes up in a number of subbands in the area of resonance. Secondly, absorption is maximum at one edge and drops almost to zero at the other edge of the subband. This is true for all subbands except the resonant. While before the resonance absorption monotonously goes down from the lower edge to the upper, after the resonance the picture become reversed. Matching the picture with Fig. 2, we see that when absorption is maximum, the final wave function has 'proper' parity, i.e. the opposite to the parity of the ground state. In the resonant band parity is 'proper' on both band edges, and band absorption spectrum has different shape.

The picture reflects the hybrid structure of the electronic spectrum of the considered

spectrum is formed mainly by barrier levels. An 'intrusion' of the resonant level from the well confuses the monotonous pattern and upturns parity switching order.

Absorption Strength

Using the momentum matrix element data shown above one can easily calculate such physical quantity of interest as the absorption probability due to the electron transition from the ground subband to a higher subband n. The standard perturbative approach for a transition probability at one photon absorption (see, for example, [12, 13]) gives the absorption probability as

$$\begin{aligned} W_{fi} &= \frac{2\pi}{\hbar}|\hat{H}^{int}_{fi}|^2\delta(\varepsilon_f-\varepsilon_i-\hbar\omega) = \frac{2\pi e^2}{m^2c^2\hbar}A_0^2\,|p_{fi}|^2\delta(\varepsilon_f-\varepsilon_i-\hbar\omega) \qquad (4)\\ &= \left(\frac{2\pi e}{m}\right)^2\frac{N(\omega)}{\omega c}\,|p_{fi}|^2\delta(\varepsilon_f-\varepsilon_i-\hbar\omega) = \left(\frac{2\pi e}{m}\right)^2\frac{I(\omega)}{\hbar\omega^2 c}\,|p_{fi}|^2\delta(\varepsilon_f-\varepsilon_i-\hbar\omega), \end{aligned}$$

where subscripts i, f stand for initial and final state, respectively; $\hat{H}^{int} = -(e/mc)\,\mathbf{A}\hat{\mathbf{p}}$ is the interaction Hamiltonian with electromagnetic field, $\mathbf{A}$ being the vector potential of the latter with the amplitude $A_0(\omega)$, and $\hat{\mathbf{p}}$ being the electron momentum operator; the photon flux density $N(\omega)$ satisfies the relation $A_0^2(\omega) = (2\pi\hbar c/\omega)N(\omega)$; $I(\omega) = \hbar\omega N(\omega)$ is the radiation spectral intensity. It was assumed in eq. (4) that the superlattice length is small as compared with the radiation wavelength, which seems reasonable for the infrared intraband transitions considered here.

On the other hand, as the superlattice we consider is not too long, we will assume that each subband Bloch level can be spectrally resolved separately from others. Assuming also that the light beam spectral width covers only one possible transition from a Bloch state in the ground subband into another Bloch state in an excited subband, after the integration over the incident radiation frequency one obtains, taking into account also the initial and final electron state degeneracy due to the perpendicular (in-plane) electron motion[1]:

$$W(\omega_{fi}) = 2\sum_{k_y,k_z}\mathcal{P}\,\left(\frac{2\pi e}{m}\right)^2\frac{I(\omega_{fi})}{\hbar^2\omega_{fi}^2 c}\,|p_{fi}|^2, \qquad (5)$$

where $\omega_{fi} = (\varepsilon_f-\varepsilon_i)/\hbar$ is the transition frequency, and $\mathcal{P}$ is the statistical factor describing the electron Fermi distribution in the ground subband. The electron momentum conservation at an optical transition has been taken into account in this equation. The factor 2 reflects the spin degeneracy.

Performing the elementary summation in eq. (5), one comes finally to the expression for the light absorption probability at the electron transition between two Bloch subband states, one in the ground subband and the other in an excited one:

$$W(\omega_{fi}) = \frac{2\pi}{c}\left(\frac{e}{\hbar^2\omega_{fi}m}\right)^2 I(\omega_{fi})\,p_{F\perp}^2\,|p_x|^2 = \left(\frac{2\pi e}{\hbar\omega_{fi}m}\right)^2\frac{I(\omega_{fi})}{c}\,\frac{N_{2d}}{\mathcal{N}}\,|p_x|^2, \qquad (6)$$

where $p_{F\perp}$ is the 2d in-plane Fermi momentum of electrons in the ground subband; N_{2d} is the corresponding sheet electron density in the superlattice; $\mathcal{N}$ is the number of the periods

[1]The degeneracy is connected with the neglect of the electron effective mass difference in the layers of the superlattice. As a result, the in-plane energy dispersion laws are similar in all subbands. This is true in doped superlattices and an approximation in compositional ones.

parallel to the growth axis x to ensure maximum absorption.

The formula (6) clearly shows that the absorption strength is proportional to $|p_z|^2$ and hence reflects all the peculiarities of the matrix element discussed above. Other physical quantities such as the cross section of the photon absorption, absorption coefficient etc. can be calculated similarly [6].

Of course, in a real superlattice the distinct absorption peaks of different subbands will blur to some extent. First, the coherence of superlattice cells deteriorates due to interface roughness and unavoidable fluctuations of layer thickness, so that k, strictly saying, fails to remain a good quantum number. The difference between the effective masses in barriers and wells, which we neglected for the sake of simplicity, should also widen the peaks.

Comparison with Properties of a Single Well

Analytic calculations have been performed in [6] for a single well heterostructure with the same model potential as in eq. (1). One could expect that the current results should fit to the conclusions of [6] in the limit of remote wells, i.e. for a long-period superlattice with $b/a \gg 1$.

We can employ $|p_n|^2\rho$ as a variable characterising optical absorption per one electron in a single quantum well, where $|p_n|^2$ is the momentum matrix element squared, and ρ is the density of final states. An analogous parameter for a superlattice is $\langle|p_n|^2\rangle/(E_n - E_{n-1})$, where $\langle\ldots\rangle$ stands again for averaging over the states in n-th subband, and E_n is the energy of the middle state in the subband (when $kb = \pi/2$). Thus $(E_n - E_{n-1})$ is approximately the distance between adjacent bands. This parameter characterises the absorption in the area of n-th subband, averaged over an energy interval. As it is evident from Fig. 4, the two variables coincide reasonably well already at $b/a = 10$.

CONCLUSIONS

We considered a superlattice with a unit cell allowing for resonant states. In this system, the dipole matrix element of the transitions between the lowest subband and one of the excited subbands significantly increases when the final subband approaches the energy of the resonant state, peaking up in the resonant subband. However, transitions to all subbands except the resonant one have a zero matrix element at one of the subband edges. The intraband absorption strength will demonstrate similar behaviour. The shape of the absorption peak corresponding to the resonant subband is strongly affected by the 'intrusion' of the quasi-localised states into the superlattice spectrum.

ACKNOWLEDGEMENTS

We acknowledge partial support of the Russian Foundation for Basic Research (through grants 96-15-96500 and 97-02-17334) and of the Foundation "Universities of Russia: Basic Research".

REFERENCES

1. V.P. Kaidanov and Yu.I. Ravich, Uspekhi Fiz. Nauk **145**, p. 51 (1985).

2. R.W. Pohl, *Einführung in die Optik* (Springer, Berlin u.a., 1948), §122.

1944), §15.

4. S.D. Beneslavskii, A.V. Dmitriev, and N.S. Salimov, JETP **92**, p. 305 (1987).
5. A.V. Dmitriev, Solid State Commun. **74**, p. 237 (1990).
6. A.V. Dmitriev, R. Keiper, and V.V. Makeev, Semiconductor Sci. and Technol. **11**, p. 1791 (1996).
7. B.F. Levine, J. Appl. Phys. **74**, p. R1 (1993).
8. G. Bastard, Phys. Rev. B **24**, p. 5693 (1981).
9. G. Bastard, Phys. Rev. B **25**, p. 7584 (1982).
10. Hung-Sik Cho and P.L. Prucnal, Phys. Rev. B **36**, p. 3237 (1987).
11. S. Flügge, *Practical Quantum Mechanics, I and II* (Springer, Berlin u.a., 1971).
12. See [3], §10.
13. H.A. Bethe, *Intermediate Quantum Mechanics* (Benjamin, New York—Amsterdam, 1964), chap. 12.